Advances in Applied Mathematics and Mechanics
Adv. Appl. Math. Mech., Vol. **3**, No. 3, pp. 297-309

DOI: 10.4208/aamm.10-10s2-03
June 2011

Comparisons of Heat Transfer Enhancement of an Internal Blade Tip with Metal or Insulating Pins

Gongnan Xie[1,2] and Bengt Sundén[2,*]

[1] *The Key Laboratory of Contemporary Design and Integrated Manufacturing Technology, Northwestern Polytechnical University, Xi'an 710072, Shaanxi, China*
[2] *Division of Heat Transfer, Lund University, SE-22100, Lund, Sweden*

Received 26 November 2009; Accepted (in revised version) 20 September 2010
Available online 28 February 2011

Abstract. Cooling methods are needed for turbine blade tips to ensure a long durability and safe operation. A common way to cool a tip is to use serpentine passages with 180-deg turn under the blade tip-cap taking advantage of the three-dimensional turning effect and impingement like flow. Improved internal convective cooling is therefore required to increase the blade tip lifetime. In the present study, augmented heat transfer of an internal blade tip with pin-fin arrays has been investigated numerically using a conjugate heat transfer method. The computational domain includes the fluid region and the solid pins as well as the tip regions. Turbulent convective heat transfer between the fluid and pins, and heat conduction within pins and tip are simultaneously computed. The main objective of the present study is to observe the effect of the pin material on heat transfer enhancement of the pin-finned tips. It is found that due to the combination of turning, impingement and pin-fin crossflow, the heat transfer coefficient of a pin-finned tip is a factor of 2.9 higher than that of a smooth tip at the cost of an increased pressure drop by less than 10%. The usage of metal pins can reduce the tip temperature effectively and thereby remove the heat load from the tip. Also, it is found that the tip heat transfer is enhanced even by using insulating pins having low thermal conductivity at low Reynolds numbers. The comparisons of overall performances are also included.

AMS subject classifications: 76D17, 80A20, 35Q80.

Key words: Heat transfer enhancement, tip-wall, pins, thermal conductivity, weight.

1 Introduction

Numerical simulations are effective means to investigate the details of fluid flow and heat transfer characteristics resulting from augmented surfaces. During recent years,

*Corresponding author.
URL: `http://www.ht.energy.lth.se/personal/bengt_sunden`
Email: xgn@nwpu.edu.cn (G. N. Xie), Bengt.Sunden@energy.lth.se (B. Sundén)

application of so-called *Computational Fluid Dynamics* (CFD) techniques to predict the flow field and heat transfer coefficient distribution in turbomachineries has attracted many researchers [1–6]. For examples, Hwang et al. [1] predicted turbulent heat transfer in a rotating two-pass channel using a modified two-equation $k-\varepsilon$ turbulence model. Chen et al. [2] calculated the 3D flow and heat transfer in a rotating two-pass square channel with smooth walls or $45^\circ/60^\circ$ angled ribs by a second-moment closure model and a two-layer $k-\varepsilon$ isotropic eddy viscosity model. Iacovides and Raisee [3] computed fluid flow and heat transfer in 2D rib-roughened passages using modified low-Re differential second-moment (DSM) closure turbulence models. Nonino and Comini [4] computed 3D laminar forced convective heat transfer in ribbed square channels by using the velocity-pressure coupling algorithm SIMPLER. The work was based on the finite element method. Jia et al. [5] and Sunden et al. [6] numerically studied turbulent heat transfer and/or impingement cooling in rib-roughened ducts using the in-house code CALC-MP. From the above-mentioned references, it is indicated that heat transfer and cooling in gas turbine channels might be predicted effectively by CFD simulations with various computational approaches.

For turbine blades in particular operation, the hot leakage flow results in high thermal loads on the blade tip. It is therefore essential to cool the turbine blade tip and the region near the tip. A common way to cool the blade tip is to adopt internal cooling by designing serpentine (two-pass, three-pass or multi-pass) channels with a 180-deg turn/bend inside the blade (as shown in Fig. 1). Taking the advantage of impinging and turning effects, the tip can be cooled to some certain extent. Consequently, augmented internal convective cooling is required to increase the blade tip life. Fortunately, it is well documented that many augmented devices, i.e., fins, ribs, pins, dimples, can be used to improve the heat transfer significantly. Many previous investigations have proven that pin-fins can improve the cooling in low aspect ratio channels for gas turbines, typically at the trailing edges. The application of pin-fins has received considerably attention for enhancing heat transfer in cooling channels, e.g., turbine blades, heat sinks, compact heat exchangers. Metzger et al. [7] studied developing heat transfer in rectangular ducts having short pin-fin arrays. They found

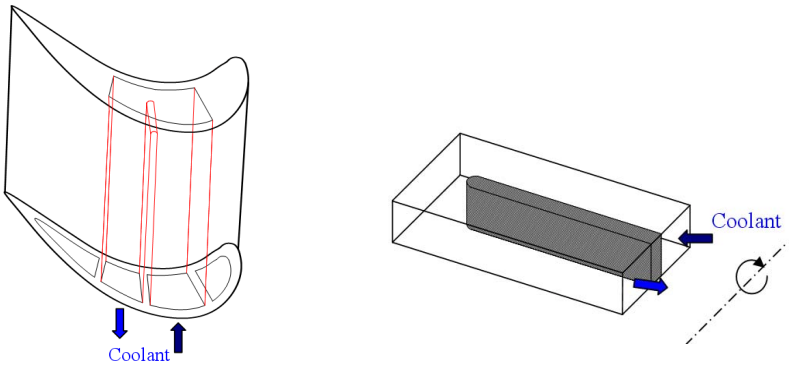

Figure 1: A typical serpentine passage inside a turbine blade.

that the heat transfer coefficient gradually increased to the first three or four rows followed by a gradual decrease through the remaining rows. Lau et al. [8] studied the effects of several pin configurations on the local endwall heat/mass transfer in pin-finned channels. They observed that the decrease of the streamwise pin spacing resulted in an increase of the endwall heat/mass transfer. Chyu et al. [9] reported that the pin-fin heat transfer is 10 to 20% higher than the endwall heat transfer. Goldstein et al. [10] found that a stepped-diameter circular pin-fin array provided a higher mass transfer coefficient and a smaller pressure loss than a uniform-diameter circular pin-fin array. Other recent investigations can be found in references [11–15]. Previous works showed that the increase in the pin-fin heat transfer is always accompanied by a substantial increase in pressure loss. Most recently, Bunker [16] presented a method to increase the convective heat transfer on an internal cooled blade tip-cap, where arrays of discrete shaped pins were placed. It was found that the effective heat transfer coefficient could be increased up to a factor of 2.5 while the tip turn pressure drop was negligible compared to that of a smooth surface.

Even though similar heat transfer results in two-pass channels with pin-fins can be found in the experimental work by Bunker [16] and numerical simulations by the authors [17–21], limited details of the heat transfer and flow field on the pin-fins and tip-walls are available. Furthermore, most previous studies were concerned about the heat transfer on the leading or/and trailing walls of two-pass channels, and thus very limited information is available for tip walls. Besides, few comprehensive studies focused the pin materials on augmented tip heat transfer, thus the main objective of the present study is to investigate the effect of pin material on heat transfer enhancement over pin-finned tips in a rectangular two-pass channel at high Reynolds number. Detailed temperature distributions are presented, and the overall performances of pin-finned-tip two-pass channels are compared and evaluated.

2 Description of physical models

A schematic diagram of the geometrical models considered in this study is provided in Fig. 2. The two-pass channels have rectangular cross-section with an aspect ratio of 1:2 with the hydraulic diameter of 93.13mm. The full tip-wall cap section is 139.7mm by 165.1mm. The tip clearance is 88.9mm. The lengths of the smooth first-pass and the smooth second-pass are about ten hydraulic diameters. Fig. 2(a) shows the smooth-tip two-pass channel. It is used for performance comparison with the pin-finned-tip two-pass channel as shown in Fig. 2(b). The numerical models of the rectangular two-pass channels are similar to those in the experiments by Bunker [16] except for the

Table 1: Material properties for the computations.

Material	Cooper	Aluminum	Titanium	Renshape	Wood	Air
Density, kg/m^3	8978	2719	4500	1800	700	1.17
Specific Heat, J/(kg·K)	381	871	522	1180	2310	1005
Thermal conductivity, W/(m·K)	387.6	202.4	21.9	1	0.173	0.027

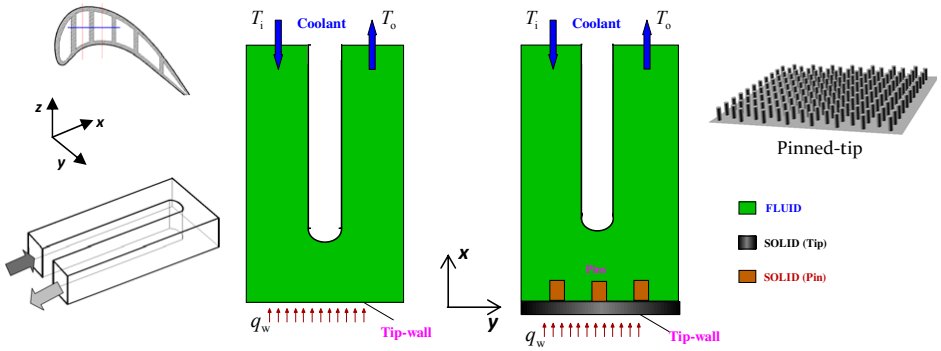

(a) smooth-tip channel (b) pin-finned-tip channel

Figure 2: Schematics of the computational models.

outlet, but the pin-fin configurations and arrangements in the present study and the experiments are different. In Fig. 2(b), pin-fin arrays are mounted on the tip, and the pin-fins are in staggered arrangement. The pins have height of 8.128mm and diameter of 4.064mm. The streamwise pitch is 21.117mm and spanwise pitch is 6.096mm. The total number of pin-fins is 165. In all simulations, the pin-fins are assumed to be perfectly circular without base-fillet or tip-radius. Five kinds of pin materials are considered in this study: copper, aluminum, titanium, wood and renshape. The former three pins are metallic while the last two pins are insulating. The use of insulating pins results in a substantially reduced tip weight, which is a key point in some certain tip designs. The material properties of the pins and fluid are listed in Table 1.

3 Computational method

In the present study, the simulation software FLUENT version 6.3.26 was used. This code uses the finite volume method to solve the governing equations of fluid flow and heat transfer with appropriate boundary conditions. The coupling of the pressure and velocity fields is handled by the SIMPLEC algorithm. Another commercial software GAMBIT version 2.4.6 providing geometry generation, geometry import and mesh generation capabilities was used to set up the computational models. Based on previous studies [19–21], the realizable $k-\varepsilon$ turbulence model is selected for all computations.

3.1 Governing equations

The governing equations of fluid flow and heat transfer for different variables can be expressed as follows [22].

- Continuity equation

$$\frac{\partial u_j}{\partial x_j} = 0. \tag{3.1}$$

• Momentum equations

$$\rho\frac{\partial u_i u_j}{\partial x_j} = -\frac{\partial p}{\partial x_i} + \frac{\partial}{\partial x_j}\Big((\mu+\mu_t)\Big(\frac{\partial u_j}{\partial x_i}+\frac{\partial u_i}{\partial x_j}\Big)\Big). \tag{3.2}$$

• Energy equation for fluid

$$\frac{\partial u_i T}{\partial x_i} = \frac{\partial}{\partial x_i}\Big(\Big(\frac{\mu}{\mathrm{Pr}}+\frac{\mu_t}{\mathrm{Pr}_t}\Big)\frac{\partial T}{\partial x_i}\Big). \tag{3.3}$$

• Energy equation for solid

$$0 = \frac{\partial}{\partial x_i}\Big(\frac{\lambda}{c_p}\frac{\partial T}{\partial x_i}\Big). \tag{3.4}$$

• Turbulent kinetic energy k equation

$$\frac{\partial}{\partial x_j}(\rho u_j k) = \frac{\partial}{\partial x_j}\Big[\Big(\mu+\frac{\mu_t}{\sigma_k}\Big)\frac{\partial k}{\partial x_j}\Big] + \Gamma - \rho\varepsilon. \tag{3.5}$$

• Rate of energy dissipation ε equation

$$\frac{\partial}{\partial x_j}(\rho u_j \varepsilon) = \frac{\partial}{\partial x_j}\Big[\Big(\mu+\frac{\mu_t}{\sigma_\varepsilon}\Big)\frac{\partial \varepsilon}{\partial x_j}\Big] + C_1\Gamma\varepsilon - C_2\frac{\varepsilon^2}{k+\sqrt{\nu\varepsilon}}, \tag{3.6}$$

where Γ represents the production rate of k and is calculated by

$$\Gamma = -\overline{u_i u_j}\frac{\partial u_i}{\partial x_j} = \nu_t\Big(\frac{\partial u_i}{\partial x_j}+\frac{\partial u_j}{\partial x_i}\Big)\frac{\partial u_i}{\partial x_j}, \tag{3.7a}$$

$$\mu_t = \rho C_\mu \frac{k^2}{\varepsilon}. \tag{3.7b}$$

The coefficients in the turbulence model are

$$C_1 = \max\Big\{0.43, \frac{\mu_t}{\mu_t+5}\Big\}, \quad C_2 = 1.0, \quad \sigma_k = 1.0, \quad \sigma_\varepsilon = 1.2.$$

3.2 Boundary conditions

The heat transfer enhancement of pin-finned tip-walls compared to a smooth tip-wall is the major concern of this paper. Therefore, except for the bottom tip wall (external smooth tip-wall), the remaining walls are assumed to be adiabatic. In order to approach the experimental conditions by Bunker [16] that uniform heat flux was created by a heater, a constant heat flux is prescribed on the bottom wall. No-slip velocity conditions are applied at all walls. Uniform inlet velocity and temperature, i.e., 300K, are set at the inlet while an outflow condition is chosen at the outlet. Due to the conjugated approach in the analysis of the heat transfer in the fluid and solid [20, 21], the

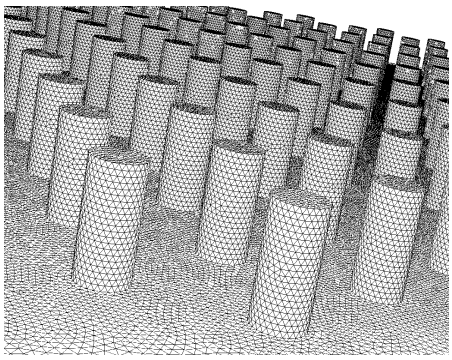

Figure 3: Typical grid distribution on pin-finned surfaces.

boundary conditions at the interfaces of fluid-solid and solid-solid are automatically handled.

The fluid is assumed to be incompressible with constant thermal physical properties and the flow is assumed to be three dimensional, turbulent, steady and non-rotating. The working fluid is dry air. In this study, because of high Reynolds numbers and complicated computational model, the standard wall functions of the Realizable $k-\varepsilon$ model are applied on the walls for the near wall treatment. The minimum convergence criterion for continuity, momentum equations, and k and ε equations are 10^{-4} while it is 10^{-7} for the energy equation.

3.3 Grid dependence

A careful check of the grid influence of the numerical solutions have been carried out by considering four grid systems with large numbers of grid points. Based on previous tests [19–21], to save computer resources and keeping a balance between computational economy and prediction accuracy, a grid of mixed 2.5M cells has been chosen for all compuations. A typical regional uniform grid distribution for all computations is shown in Fig. 3. These simulations are performed on a PC with two CPUs having a frequency of 3.0 GHz and a core memory of 8G. Typical running times for computation of one case is about 48 hours for the pin-finned tip channels.

4 Results and discussion

4.1 Parameter definitions

Before analysing and comparing the fluid flow and heat transfer characteristics, the Nusselt number and friction factor definitions are provided. First, the Fanning friction factor f is defined as

$$f=\frac{\Delta p}{2\rho u_i^2}\cdot\frac{D_h}{L}, \tag{4.1}$$

where u_i is the inlet velocity, L is the two-pass channel total length.

The overall/averaged Nusselt number can be calculated in the following way. The local Nusselt numbers of every cell vertices are first calculated by

$$Nu(i) = \frac{q_w}{T(i) - T_f} \cdot \frac{D_h}{\lambda}, \tag{4.2}$$

where T_f is the mass-weighted average value of the inlet and outlet fluid temperatures, and $T(i)$ is the local temperature of every cell at the surfaces. The overall Nusselt number is determined by area-weighted averaging of all local Nusselt numbers including those on the bottom wall.

4.2 Model validation

The turbulent flow and heat transfer in the smooth-tip channel have been computed so that the averaged Nusselt number and pressure drop can be compared with those in the related experiments [16]. Decent overall agreement between the predicted and experimental results ensures the reliability of the physical model and computational method. More details can be found in [20, 21].

4.3 Temperature distributions

The flow fields inside the two-pass channels are not given in this paper but can be found in [17–21]. For showing the effects of the pin material, the temperature distributions of the various tips are presented in Fig. 4. In general, the tips with metal pins

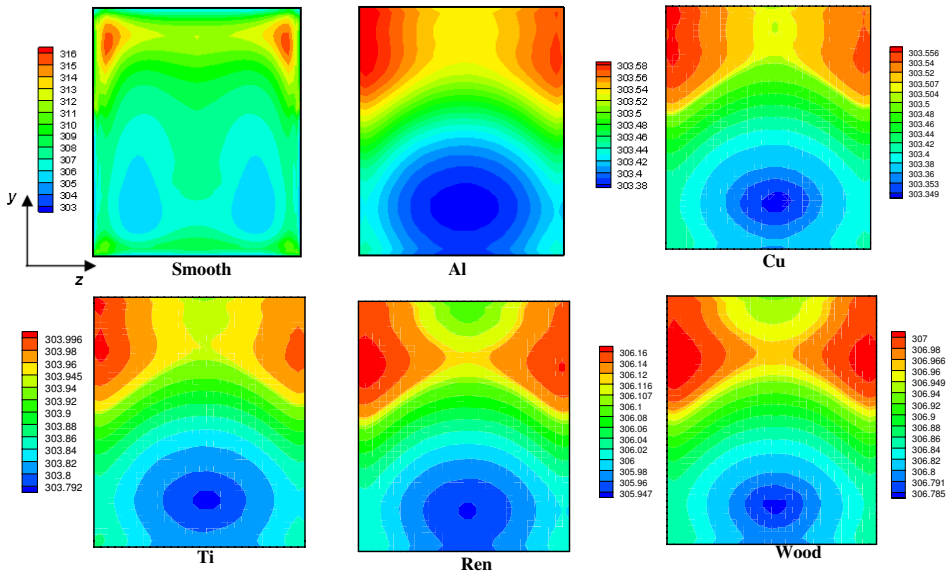

Figure 4: Typical temperature distributions at $Re = 200,000$ (unit: K).

have lower temperature everywhere compared to the tips with insulating pins. This indicates that metal pins can remove the heat load from the tips effectively leading to a lower surface temperature. Also, by comparing the smooth-tip temperature distribution, the augmented-tips have lower and more uniform temperature distributions because of pin-fin crossflow and tip conduction.

4.4 Heat transfer and pressure drop

The surface averaged/overall Nusselt number and inlet-outlet pressure drop for all Reynolds numbers are summarized in Fig. 5. From Fig. 5(a), the tip with *Cu* pins offers the highest Nusselt number especially at high Reynolds numbers, while the tip with wood pins offers the lowest Nusselt number. As the thermal conductivity increases, the increase of the heat transfer is decreased, i.e., *Cu* pins have no significant enhancement compared to *Al* pins. This means that for agumenting tip heat transfer it is not necessary to adopt those pins with very high thermal conductivity. At $Re = 600,000$, tip with wood pins offers 6% smaller heat transfer than the smooth-tip. Part of this deviation might be due to precision in the computations. For the pressure loss, the pin-finned tips produce about 10% higher pressure drop at high Reynolds number, i.e., 600,000. As expected, for augmented tips, the pressure drops do not depend on the pin material, as the pin configuration and arrangement are identical.

The individual fin efficiencies of all pins and heat transfer enhancements are provided in Fig. 6. It can be seen from Fig. 6(a) that the fin efficiency decreases with increasing Reynolds number. The tip with *Cu* or *Al* pins offers higher fin efficiency close to unity because *Cu* or *Al* has a large thermal conductivity. The tip with wood pins provides the smallest fin efficiency of about 10∼20%. The tip with titanium pins provides a moderate fin efficiency of about 71∼85%. From Fig. 6(b), the heat transfer enhancement over the smooth tip decreases with increasing Reynolds number. At low Reynolds number, the tips with *Cu* and *Al* pins produce the highest heat transfer en-

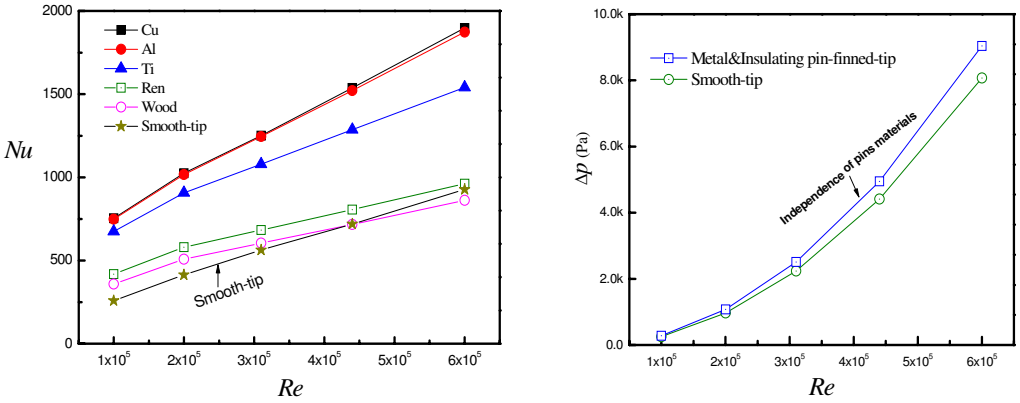

(a) Nusselt number (b) Pressure drop

Figure 5: The averaged Nusselt number and pressure drop for all Reynolds numbers.

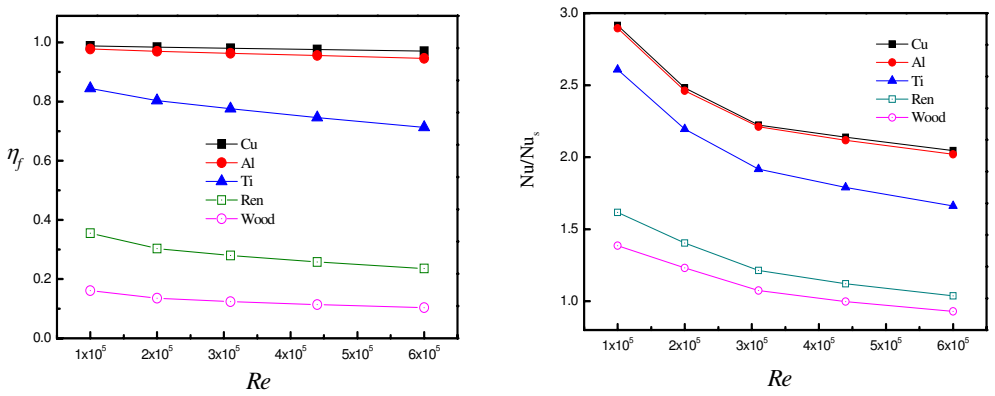

(a) Fin efficiency (b) Nusselt number ratio

Figure 6: The pin fin efficiency and heat transfer enhancement.

hancement, i.e., a factor of 2.9. At high Reynolds number, the tip with wood pins does not show significant enhancement. For the tip with titanium pins, the heat transfer enhancement lies between 1.6 and 2.6. On the other hand, the tip with wood pins offers heat transfer enhancement about 1.4 times at low Reynolds number, i.e., 100,000. This indicates that adding pins with even low thermal conductivity can augment tip heat transfer and thereby improve the blade tip cooling.

5 Overall comparison

From the foregoing analysis it can be found that the two-pass channels with pin-finned tip provide higher Nusselt number associated with higher pressure drop. On the other hand, for practical operation, minimizing the blade weight is an objective for designing rotating blades. The added weight implies possible larger stresses, which result in reduced reliability and life. For these reasons it is essential to compare the heat transfer enhancement performance of the two-pass augmented tip channels. Fig. 7 presents a comparison of the overall performance using several criteria. From Fig. 7(a), it can be seen that at all Reynolds numbers, the pin-finned tips are superior to the smooth-tip except that beyond Reynolds number of 300,000 the smooth-tip is superior compared to the tip with wood pins. Since most of the heat transfer augmentation is attributed to the addition of extended area, the augmentation excluding the area enhancement factor should be evaluated. As found in Fig. 7(b), by disregarding the increased active heat transfer area, the tips with *Cu* or *Al* pins produce 15∼26% higher heat transfer enhancement than a wood pin-tip. The insulating *Ren* pin-tip is superior compared to the metal *Ti* pin-tip. Compared to a wood pin-tip, the renshape pin-tip produces 11∼16% higher enhancement while 2∼8% higher enhancement is produced by the titanium pin-tip. Note that for the metal pins, the internal pin-finned tip surface area enhancement factor is 1.74 compared to the smooth-tip surface area while for the insulating pins the corresponding factor is unity.

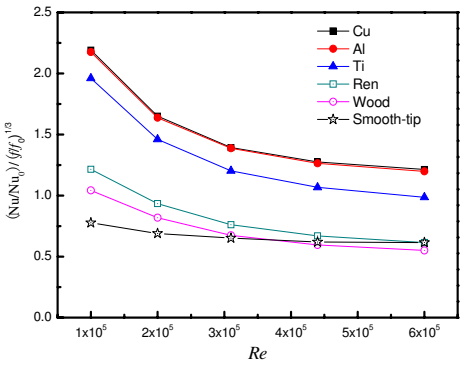

(a) $(Nu/Nu_0)/(f/f_0)^{1/3}$

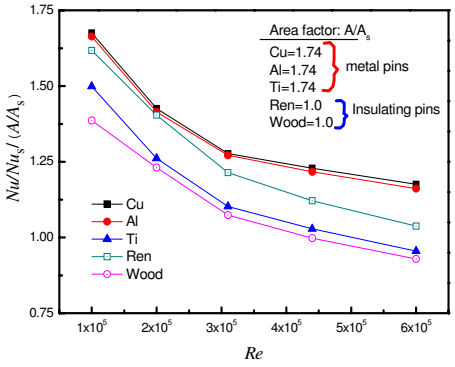

(b) Enhancement excluding area enhancement factor

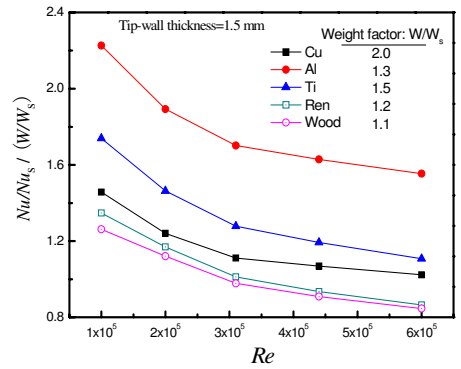

(c) Enhancement excluding pin weight, *Ti* tip

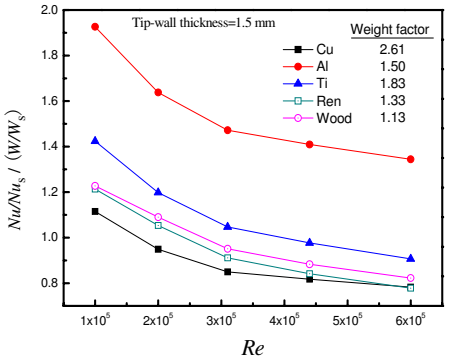

(d) Enhancement excluding pin weight, *Al* tip

Figure 7: The pin fin performance and heat transfer enhancement.

Weight is a factor that must be considered in the blade design. Therefore the overall performance should be evaluated with tip weight constraint. First the material of the plane tip is assumed to be *Ti* with a thickness of 1.5mm. The Nusselt number ratios normalized by the weight ratios are plotted in Fig. 7(c). It is found that *Al*, *Ti* and *Cu* pin-tips produce 68∼73%, 30∼38% and 10∼21% higher heat transfer enhancement than a wood pin-tip, respectively. Renshape pin-tip produces 2∼7% higher enhancement. Secondly the material of the plane tip is assumed to be *Al* with a thickness of 1.5mm. As shown in Fig. 7(d), by disregarding the factor of the increased weight, it is found that *Al* and *Ti* pin-tips produce around 72% and 16∼28% higher heat transfer enhancement than a *Cu* pin-tip, respectively. The *Ren* and wood pin-tip produce up to 21% and 15% higher enhancement than a *Cu* pin-tip at low Reynolds numbers, respectively.

6 Conclusions

Three-dimensional turbulent flow and convective heat transfer over pin-finned tips in rectangular two-pass channels have been numerically investigated. The effect of the

pin material on the tip heat transfer is studied. The main findings from this study are summarized as follows:

1. By using metal pins with large thermal conductivity, the tip temperature can be significantly reduced and hence the tip cooling is enhanced.
2. The relative augmentation of heat transfer decreases with increasing thermal conductivity of the pins. This suggests that it is not necessary to use pins having extremely high thermal conductivity.
3. Compared to the smooth-tip channel, the heat transfer enhancement of the pin-finned-tip channel is up to a factor of 2.9 associated with less than 10% higher pressure loss. The larger the thermal conductivity of the pins is, the higher is the tip heat transfer. At low Reynolds numbers, the tip heat transfer is enhanced even by using insulating pins with a low thermal conductivity.
4. It is found that the pin-finned tip channel provides good overall performance. When pin-fins are used to enhance the tip cooling, the heat transfer enhancement should be evaluated with respect to the balance between cooling efficiency and active area, tip weight, especially when metal pins are used.

Acknowledgements

The research has been funded by the Swedish Energy Agency, Siemens Industrial Turbomachinery AB and Volvo Aero Corporation through the Swedish research program TURBO POWER, the support of which is gratefully acknowledged.

Nomenclature

A	tip-wall surface area
D_h	hydraulic diameter
f	Fanning friction factor
h	heat transfer coefficient
k	turbulent kinetic energy
L	length of two-pass channel
Nu	Nusselt number
Pr	Prandtl number
p	pressure
q_w	wall heat flux
Re	Reynolds number, $Re = \rho u_i D_h / \mu$
T	temperature
u_i	inlet velocity
W	tip weight

Greek symbols

ε	Rate of energy dissipation
η_f	fin efficiency
Δp	pressure drop
λ	fluid thermal conductivity
μ	fluid dynamic viscosity
ρ	fluid density

Subscripts

0	fully developed flow channel
f	fluid
i	inlet
o	outlet
s	smooth-tip channel

References

[1] J. J. HWANG, T. Y. LIA, AND S. H. CHEN, *Prediction of turbulent fluid flow and heat transfer in a rotating periodical two-pass square duct*, Int. J. Numer. Methods. Heat. Fluid. Flow., 8 (1998), pp. 519–538.

[2] H. C. CHEN, Y. J. JANG, AND J. C. HAN, *Computation of heat transfer in rotating two-pass square channels by a second-moment closure model*, Int. J. Heat. Mass. Trans., 43 (2000), pp. 603–616.

[3] H. IACOVIDES, AND M. RAISEE, *Computation of flow and heat transfer in two-dimensional rib-roughened passages using low-Reynolds-number turbulence models*, Int. J. Numer. Methods. Heat. Fluid. Flow., 11 (2001), pp. 138–155.

[4] C. NONINO, AND G. COMINI, *Convective heat transfer in ribbed square channel*, Int. J. Numer. Methods. Heat. Fluid. Flow., 12 (2002), pp. 610–628.

[5] R. JIA, M. ROKNI, AND B. SUNDÉN, *Impingement cooling in a rib-roughened channel with cross-flow*, Int. J. Numer. Methods. Heat. Fluid. Flow., 11 (2001), pp. 642–662.

[6] B. SUNDÉN, R. JIA, AND A. ABDON, *Computation of combined turbulent convective and impingement heat transfer*, Int. J. Numer. Methods. Heat. Fluid. Flow., 14 (2004), pp. 116–133.

[7] D. E. METZGER, R. A. BERRY, AND J. P. BRONSON, *Developing heat transfer in rectangular ducts with staggered arrays of short pin fins*, ASME J. Heat. Trans., 104 (1982), pp. 700–706.

[8] S. C. LAU, Y. S. KIM, AND J. C. HAN, *Local endwall heat/ mass distributions in pin fin channels*, AIAA J. Thermophys., 1 (1987), pp. 365–372.

[9] M. K. CHYU, Y. C. HSING, T. I. P. SHIH, AND V. NATARAJAN, *Heat transfer contributions of pins and endwall in pin-fin arrays: effect of thermal boundary condition modelling*, ASME J. Turbomachinery., 121 (1999), pp. 257–263.

[10] R. J. GOLDSTEIN, M. Y. JABBARI, AND S. B. CHEN, *Convective mass transfer and pressure loss characteristics of staggered short pin-fin arrays*, Int. J. Heat. Mass. Trans., 37 (1994), pp. 149–160.

[11] L. M. WRIGHT, E. LEE, AND J. C. HAN, *Effect of rotating on heat transfer in rectangular channels with pin fins*, AIAA J. Thermophys. Heat. Trans., 18 (2004), pp. 263–272.

[12] F. E. AMES, L. A. DVORAK, AND M. J. MORROW, *Turbulent augmentation of internal convection over pins in staggered-pin fin arrays*, ASME J. Turbomachinery., 127 (2005), pp. 183–190.

[13] N. SAHITI, A.LEMOUEDDA, D. STOJKOVIC, F. DURST, AND E. FRANZ, *Performance comparison of pin fin in-duct flow arrays with various pin cross-section*, Appl. Thermal. Eng., 26 (2006), pp. 176–1192.

[14] G. G. SU, H. C. CHEN, AND J. C. HAN, *Computation of flow and heat transfer in rotating rectangular channels ($AR = 4 : 1$) with pin-fins by a Reynolds stress turbulence model*, ASME J. Heat. Trans., 129 (2007), pp. 685–696.

[15] S. W. CHANG, T. L. YANG, C. C. HUANG, AND K. F. CHIANG, *Endwall heat transfer and pressure drop in rectangular channels with attached and detached circular pin-fin array*, Int. J. Heat. Mass. Trans., 51 (2008), pp. 5247–5259.

[16] R. S. BUNKER, *The augmentation of internal blade tip-cap cooling by arrays of shaped pins*, Proceedings of GT2007, ASME Turbo 2007, paper no. GT2007-27009.

[17] G. N. XIE, B. SUNDÉN, L. WANG, AND E. UTRIAINEN, *Enhanced heat transfer on the tip-wall in a rectangular two-pass channel by pin-fin arrays*, Numer. Heat. Trans., 53 (2009), pp. 739–761.

[18] G. N. XIE, B. SUNDÉN, E. UTRAINEN, AND L. WANG, *Computational analysis of pin-fin arrays effects of internal heat transfer enhancement of a blade tip-wall*, ASME J. Heat. Trans., 132 (2010), 031901.

[19] G. N. XIE, B. SUNDÉN, L. WANG, AND E. UTRIAINEN, *Augmented heat transfer of an internal blade tip by full or partial arrays of pin-fins*, Int. Symp. Heat. Trans. Gas. Turb. Sys., 9-14 August 2009, Antalya, Turkey.

[20] G. N. XIE, AND B. SUNDÉN, *Conjugated heat transfer enhancement of an internal blade pin-finned tip*, Proceedings of 2009 ASME International Mechanical Engineering Congress and Exposition, IMECE2009, November 13-19, 2009, Lake Buena Vista, Florida, USA, paper no. IMECE2009-10296.

[21] G. N. XIE, AND B. SUNDÉN, *Conjugated analysis of heat transfer enhancement of an internal blade tip-wall with pin-fin arrays*, J. Enhanced. Heat. Trans., accepted, in press.

[22] T.-H. SHIH, W. W. LIOU, A. SHABBIR, Z. YANG, AND J. ZHU, *A new $k - \varepsilon$ eddy-viscosity model for high Reynolds number turbulent flows model development and validation*, Comput. Fluids., 24 (1995), pp. 227–238.